

Atomic Bose-Einstein Condensation with Three-Body Interactions and Collective Excitations

A. Gammal⁽¹⁾, T. Frederico⁽²⁾, Lauro Tomio⁽¹⁾ and Ph. Chomaz⁽³⁾

⁽¹⁾ *Instituto de Física Teórica, Universidade Estadual Paulista, 01405-900 São Paulo, Brazil*

⁽²⁾ *Departamento de Física, Instituto Tecnológico da Aeronáutica, Centro Técnico Aeroespacial, 12228-900 São José dos Campos, SP, Brazil*

⁽³⁾ *GANIL, B.P. 5027, F-14021 Caen Cedex, France*

(May 14, 2019)

The stability of a Bose-Einstein condensed state of trapped ultra-cold atoms is investigated under the assumption of an attractive two-body and a repulsive three-body interaction. The Ginzburg-Pitaevskii-Gross (GPG) nonlinear Schrödinger equation is extended to include an effective potential dependent on the square of the density and solved numerically for the s -wave. The lowest frequency of the collective mode is determined and its dependences on the number of atoms and on the strength of the three-body force are studied. We show that the addition of three-body dynamics can allow the number of condensed atoms to increase considerably, even when the strength of the three-body force is very small compared with the strength of the two-body force. We also observe a first-order liquid-gas phase transition for the condensed state up to a critical strength of the effective three-body force.

PACS 03.75.Fi, 42.65.Sf, 36.40.Ei, 32.80.Pj

I. INTRODUCTION

The theoretical research on Bose-Einstein condensation (BEC) [1], a phenomenon predicted more than 70 years ago, is receiving considerable experimental and theoretical support in recent years [2]. The relevance of BEC for understanding the properties of liquid ^4He was pointed out by London [3], suggesting that the peculiar phase transition that liquid helium undergoes at 2.18K is a BEC phenomenon. It is also important to observe that, at the level of two-body collisions, Bogoliubov in 1947 [4] has shown for homogeneous gas that BEC is only possible for systems with repulsive potentials.

Intense experimental researches on BEC for magnetically trapped weakly interacting atoms have been done recently [5–8]. In the experiment reported in [5], a condensate of approximately 2000 spin-polarized ^{87}Rb atoms was produced in a cylindrically symmetric magnetic trap [2,9]. It is a common understanding that, in low temperature and density, where interatomic distances are much greater than the distance scale of atom-atom interactions, two-body interactions take a simple form, and three-body interactions can be neglected. At such regime, only two-body s -wave scattering is important. With temperature low enough the magnitude of the scattering length a is much less than the corresponding thermal de Broglie wavelength, and the exact shape of two-atom interaction is unimportant.

The experimental evidences of Bose-Einstein condensation (BEC) in magnetically trapped weakly interacting atoms [5–8] brought a considerable support to the theoretical research on bosonic condensation. The nature of the effective atom-atom interaction determines the stability of the condensed state: the two-body pseudopotential

is repulsive for a positive s -wave atom-atom scattering length and it is attractive for a negative scattering length [10]. The ultra-cold trapped atoms with repulsive two-body interaction undergoes a phase-transition to a stable Bose condensed state, in several cases found experimentally, as for ^{87}Rb [5], ^{23}Na [7] and ^1H [8]. However, a condensed state of atoms with negative s -wave atom-atom scattering length (as in case of ^7Li [6]) would be unstable, unless the number of atoms N is small enough such that the stabilizing force provided by the harmonic confinement in the trap overcomes the attractive interaction, as found on theoretical grounds [11,12]. It was indeed observed in the ^7Li gas [6], for which the s -wave scattering length is $a = -14.5 \pm 0.4 \text{ \AA}$, that the number of allowed atoms in the Bose condensed state was limited to a maximum value between 650 and 1300, which is consistent with the mean-field prediction [11].

So, for systems of atoms with attractive two-body interaction, it is widely believed [11,13,14] that the condensate has no stable solution above certain critical number of atoms N_{max} . However, in this case the addition of a repulsive potential derived from three-body interaction is consistent with a number of atoms larger than N_{max} . Even for a very small strength of the three-body force, the region of stability for the condensate can be extended considerably, as previously reported in [15,16], and shown in more detail in the present work. By considering the possible effective interactions, it was reported in Ref. [17] that a sufficiently dilute and cold Bose gas exhibits similar three-body dynamics for both signs of the s -wave atom-atom scattering length. It was also suggested that, for a large number of bosons the three-body repulsion can overcome the two-body attraction, and a stable condensate will appear in the trap [18]. If

an atomic system is characterized by having effectively an attractive two-body interaction together with a repulsive three-body interaction, two mechanisms for stability are possible: (a) the kinetic energy acting at lower densities and (b) the repulsive weak three-body force effective at higher densities. These mechanisms indicate that, for the same number of atoms, one lower-density phase and a higher-density phase can be found, if the three-body force is weak enough not to dominate the effective interaction.

It was pointed out in Ref. [19] that an easier experimental approach to probe density fluctuations is to consider an observable directly sensitive to the probability of finding three atoms near each other, which will correspond to the loss rate of atoms due to three-body recombination. Such a three-body recombination rate in BEC, was considered recently in Refs. [20], [21] and [14] (see also the review of [13]). It was shown in Ref. [20] that the three-body recombination coefficient of ultracold atoms to a weakly bound s level goes to infinity in the Efimov limit [22]. The Efimov limit is a particularly interesting three-body effect, which happens when the two-body scattering length is very large (positive or negative). In this case, with the two boson energy close to zero, the three-boson system presents an increasing number of loosely bound three body states, which have large spatial extension and do not depend on the details of the interaction [23]. So, our main motivation here is to provide an extension to the GPG equation [24,25], which considers a three-body interaction and, in this way, provides the framework for a numerical investigation of the relevance of three-body interaction in Bose-Einstein condensation.

In the present work we consider a possible general scenario of atomic systems with attractive two-body and repulsive three-body interactions. By using the mean-field approximation, we investigate the competition between the leading term of an attractive two-body interaction, originated from a negative two-atom s -wave scattering length, and a repulsive three-body effective interaction, which can happen in the Efimov limit [22] ($|a| \rightarrow \infty$) as discussed in Ref. [17] *. We show that, in a dilute gas, a small repulsive three-body force added to an attractive two-body interaction is able to stabilize the condensate beyond the critical number of atoms in the trap, found just with attractive two-body force [11], such that a kind of liquid-gas phase-transition occurs. The plan of the paper is as follows. In section II, we introduce the Ginzburg - Pitaevskii - Gross (GPG) formalism. In section III, we present the main numerical results for the static solutions, together with a variational analysis. In section IV,

*The physics of three-atoms in the Efimov limit is discussed in Ref. [23], that extends a previous study of universal aspects of the Efimov effect [26].

we present a stability analysis and results for collective excitation in the condensate. In this section IV we also observe that the inclusion of three body effects points out possible evidences of a liquid - gas phase transition in the condensate. Finally, in section V, we present our main conclusions.

II. GINZBURG - PITAEVSKII - GROSS FORMALISM

In the following, we present our formalism, where the original Ginzburg - Pitaevskii - Gross (GPG) non-linear equation [24,25], which includes a term proportional to the density (two-body interaction), is extended through the addition of a term proportional to the squared-density (three-body interaction). Next, after reducing such equation to dimensionless units, we study numerically the s -wave solution by varying the corresponding dimensionless parameters, which are related to the two-body scattering length, the strength of the three-body interaction and the number of atoms in the condensed state. As particularly observed in Ref. [27], to incorporate all two-body scattering processes in such many particle system, the two-body potential should be replaced by the many-body T -matrix. Usually, at very low energies, this is approximated by the two-body scattering matrix, which is directly proportional to the scattering length [12]. So, in order to obtain the desired equation, we first consider the effective Lagrangian, which describes the condensed wave-function in the Hartree approximation, implying the GPG energy functional:

$$\mathcal{L} = \int d^3r \left[\frac{i\hbar}{2} \Psi^\dagger(\vec{r}) \frac{\partial \Psi(\vec{r})}{\partial t} - \frac{i\hbar}{2} \frac{\partial \Psi^\dagger(\vec{r})}{\partial t} \Psi(\vec{r}) + \frac{\hbar^2}{2m} \Psi^\dagger(\vec{r}) \nabla^2 \Psi(\vec{r}) - \frac{m}{2} \omega^2 r^2 |\Psi(\vec{r})|^2 \right] + \mathcal{L}_I. \quad (1)$$

In our description, the atomic trap is given by a rotationally symmetric harmonic potential, with angular frequency ω , and \mathcal{L}_I gives the effective atom interactions up to three particles.

The effective interaction Lagrangian for ultra-low temperature bosonic atoms, including two- and three-body scattering at zero energy, is written as:

$$\begin{aligned} \mathcal{L}_I = & -\frac{1}{2} \int d^3r_1 d^3r_2 d^3r'_1 d^3r'_2 \Psi^\dagger(\vec{r}'_1) \Psi^\dagger(\vec{r}'_2) \Psi(\vec{r}_1) \Psi(\vec{r}_2) \\ & \times \left\langle \vec{r}'_{12} \left| T^{(2)}(0) \right| \vec{r}_{12} \right\rangle \delta^3(\vec{r}'_1 + \vec{r}'_2 - \vec{r}_1 - \vec{r}_2) \\ & - \frac{1}{3!} \int \prod_{i=1}^3 (d^3r_i d^3r'_i \Psi^\dagger(\vec{r}'_i) \Psi(\vec{r}_i)) \delta^3(\vec{R}'_{123} - \vec{R}_{123}) \\ & \times \left\langle \vec{r}'_{12} \vec{R}'_3 \left| T^{(3)}(0) - \sum_{j < k} T_{jk}^{(2)}(0 - K_i) \right| \vec{r}_{12} \vec{R}_3 \right\rangle, \quad (2) \end{aligned}$$

where \vec{r}_{12} and \vec{R}_3 are the relative coordinates, given by $\vec{r}_{12} = \vec{r}_1 - \vec{r}_2$ and $\vec{R}_3 = \vec{r}_3 - (\vec{r}_1 + \vec{r}_2)/2$; and $\vec{R}_{123} \equiv (\vec{r}_1 + \vec{r}_2 + \vec{r}_3)$. $T^{(3)}(0)$ and $T_{jk}^{(2)}(0)$ are the corresponding three-body T -matrix and two-body T -matrix for the pair jk , which are evaluated at zero-energy. The two-body T -matrix for each pair (jk) is subtracted from $T^{(3)}(0)$ to avoid double counting and K_i is the kinetic energy operator for particle i .

We can approximate the above effective interaction Lagrangian at low densities by averaging the T -matrices over the relative coordinates, considering that the thermal wave-length is much greater than the characteristic interaction distances.

$$\begin{aligned} \mathcal{L}_I = & -\frac{1}{2} \int d^3 r'_{12} d^3 r_{12} \langle \vec{r}'_{12} | T^{(2)}(0) | \vec{r}_{12} \rangle \int d^3 r |\Psi(\vec{r})|^4 \\ & - \frac{1}{3!} \int d^3 r'_{12} d^3 R'_3 d^3 r_{12} d^3 R_3 \int d^3 r |\Psi(\vec{r})|^6 \\ & \times \left\langle \vec{r}'_{12} \vec{R}'_3 \left| T^{(3)}(0) - \sum_{j < k} T_{jk}^{(2)}(0 - K_i) \right| \vec{r}_{12} \vec{R}_3 \right\rangle. \end{aligned} \quad (3)$$

The integrations of the T -matrices over the relative coordinates gives the zero momentum matrix elements:

$$\begin{aligned} & \int d^3 r'_{12} d^3 r_{12} \langle \vec{r}'_{12} | T^{(2)}(0) | \vec{r}_{12} \rangle = \\ & (2\pi)^3 \langle \vec{p}_{12} = 0 | T^{(2)}(0) | \vec{p}_{12} = 0 \rangle = \frac{4\pi\hbar^2 a}{m}, \end{aligned} \quad (4)$$

where a is the two-body scattering length. For the connected three-body T -matrix, also by integrating over the coordinates, we obtain the corresponding zero momentum ($\vec{p}_{12} = 0, \vec{P}_3 = 0$) matrix elements, which give us the strength of the three-body effective interaction λ_3 , as follows:

$$\begin{aligned} & \int d^3 r'_{12} d^3 R'_3 d^3 r_{12} d^3 R_3 \\ & \times \left\langle \vec{r}'_{12} \vec{R}'_3 \left| T^{(3)}(0) - \sum_{j < k} T_{jk}^{(2)}(0 - K_i) \right| \vec{r}_{12} \vec{R}_3 \right\rangle = \\ & = (2\pi)^6 \left\langle \left| T^{(3)}(0) - \sum_{j < k} T_{jk}^{(2)}(0 - K_i) \right| \right\rangle \\ & = 2\lambda_3, \end{aligned} \quad (5)$$

where $\langle | \equiv \langle \vec{p}_{12} = 0, \vec{P}_3 = 0 |$ and $| \equiv | \vec{p}_{12} = 0, \vec{P}_3 = 0 \rangle$.

The nonlinear Schrödinger equation, which describes the condensed wave-function in the mean-field approximation, is obtained from the effective Lagrangian given in Eq. (1). By considering the interaction in Eq. (3), it can be written as [28]

$$\begin{aligned} i\hbar \frac{\partial \Psi(\vec{r}, t)}{\partial t} = & \left[-\frac{\hbar^2}{2m} \nabla^2 + \frac{m}{2} \omega^2 r^2 - N \frac{4\pi\hbar^2 |a|}{m} |\Psi(\vec{r}, t)|^2 \right. \\ & \left. + \lambda_3 N^2 |\Psi(\vec{r}, t)|^4 \right] \Psi(\vec{r}, t). \end{aligned} \quad (6)$$

For a stationary solution, $\Psi(\vec{r}, t) = e^{-i\mu t/\hbar} \psi(\vec{r})$, and the above equation can be written as

$$\begin{aligned} \mu \psi(\vec{r}) = & \left[-\frac{\hbar^2}{2m} \nabla^2 + \frac{m}{2} \omega^2 r^2 - N \frac{4\pi\hbar^2 |a|}{m} |\psi(\vec{r})|^2 \right. \\ & \left. + \lambda_3 N^2 |\psi(\vec{r})|^4 \right] \psi(\vec{r}), \end{aligned} \quad (7)$$

where μ is the chemical potential (single particle energy) and $\psi(\vec{r})$ is normalized as

$$\int d^3 r |\psi(\vec{r})|^2 = 1. \quad (8)$$

The total energy of the system is given by

$$\begin{aligned} E = & \int d^3 r \left\{ N \frac{\hbar^2}{2m} |\nabla \psi(\vec{r})|^2 + N \frac{m}{2} \omega^2 r^2 |\psi(\vec{r})|^2 \right. \\ & \left. - \frac{N^2}{2} \frac{4\pi\hbar^2 |a|}{m} |\psi(\vec{r})|^4 + \frac{N^3}{3} \lambda_3 |\psi(\vec{r})|^6 \right\}. \end{aligned} \quad (9)$$

The central density of the system can be obtained directly from the solution of the above equation, normalized as in Eq. (8):

$$\rho_c = N |\psi(0)|^2. \quad (10)$$

The physical scales presented in the above equations can be easily recognized by working with dimensionless equations. By rescaling Eq. (7) for the s -wave solution, we obtain

$$\left[-\frac{d^2}{dx^2} + \frac{1}{4} x^2 - \frac{|\Phi(x)|^2}{x^2} + g_3 \frac{|\Phi(x)|^4}{x^4} \right] \Phi(x) = \beta \Phi(x), \quad (11)$$

where $x \equiv \sqrt{2m\omega/\hbar} r$ and $\Phi(x) \equiv N^{1/2} \sqrt{8\pi|a|} r \psi(\vec{r})$. The dimensionless parameters, related to the chemical potential and the three-body strength are, respectively, given by

$$\beta \equiv \frac{\mu}{\hbar\omega} \quad \text{and} \quad g_3 \equiv \lambda_3 \hbar\omega \left[\frac{m}{4\pi\hbar^2 a} \right]^2. \quad (12)$$

The normalization for $\Phi(x)$, obtained from Eq. (8), defines a number n related to the number of atoms N :

$$\int_0^\infty dx |\Phi(x)|^2 = n, \quad \text{where} \quad n \equiv 2N|a| \sqrt{\frac{2m\omega}{\hbar}}. \quad (13)$$

The boundary conditions in Eq.(11) are given by [11]

$$\begin{aligned} \Phi(x \rightarrow 0) & \rightarrow 0 \\ \Phi(x \rightarrow \infty) & \propto \exp\left(-\frac{x^2}{4} + \left[\beta - \frac{1}{2}\right] \ln(x)\right). \end{aligned} \quad (14)$$

In terms of the dimensionless variables, the total energy of the system is given by

$$\begin{aligned} E = & \hbar\omega N \int_0^\infty dx \left\{ \left| \frac{d\phi(x)}{dx} \right|^2 + \frac{x^2 \phi^2(x)}{4} \right. \\ & \left. - \frac{n\phi^4(x)}{2x^2} + \frac{n^2 g_3 \phi^6(x)}{3x^4} \right\}, \end{aligned} \quad (15)$$

where $\phi(x) \equiv \Phi(x)/n^{1/2}$ is normalized to one.

III. LIQUID-GAS PHASE TRANSITION - STATIC SOLUTIONS

A. Variational Approach

As a further reference to our results, and the stability analysis, it will be helpful first to consider a variational procedure [29], using a trial gaussian wave function for $\psi(\vec{r})$. So, in Eq. (9) we consider the following variational wave function (normalized to one):

$$\psi_{var}(\vec{r}) = \left(\frac{1}{\pi\alpha^2} \frac{m\omega}{\hbar} \right)^{\frac{3}{4}} \exp \left[-\frac{r^2}{2\alpha^2} \left(\frac{m\omega}{\hbar} \right) \right], \quad (16)$$

where α is a dimensionless variational parameter. The corresponding root-mean-square radius, r_0 , will be proportional to the variational parameter α :

$$r_0 \equiv \sqrt{\langle r^2 \rangle_{var}} = \alpha \sqrt{\frac{3\hbar}{2m\omega}}. \quad (17)$$

The expression for the total variational energy, which is obtained after replacing Eq. (16) in Eq. (9), is given by

$$E_{var}(\alpha) = \hbar\omega N \left[\frac{3}{4} \left(\alpha^2 + \frac{1}{\alpha^2} \right) - \frac{n}{4\sqrt{\pi}\alpha^3} + \frac{2n^2g_3}{9\sqrt{3}\pi\alpha^6} \right]. \quad (18)$$

In the same way, we can obtain the corresponding variational expression for the single particle energy, Eq. (7):

$$\mu_{var}(\alpha) = \hbar\omega \left[\frac{3}{4} \left(\alpha^2 + \frac{1}{\alpha^2} \right) - \frac{n}{2\sqrt{\pi}\alpha^3} + \frac{2n^2g_3}{3\sqrt{3}\pi\alpha^6} \right]. \quad (19)$$

The variational central density, using Eqs. (10) and (16), can also be given in terms of this parameter α :

$$\rho_{c,var}(\alpha) = \left(\frac{m\omega}{\pi\hbar} \right)^{3/2} \frac{1}{\alpha^3}. \quad (20)$$

The approximate solutions for the total energy are obtained from the extrema of (18) with respect to variation of the parameter α .

The variational solutions of $E_{var}(\alpha)$ are given, as a function of n and g_3 (where $a < 0$ and $g_3 > 0$), by the real roots of $\partial E_{var}(\alpha)/\partial\alpha = 0$ [†].

[†]By using a numerical procedure one can reach easily the extrema of Eq. (18) by varying the parameter α , once the other parameters are fixed.

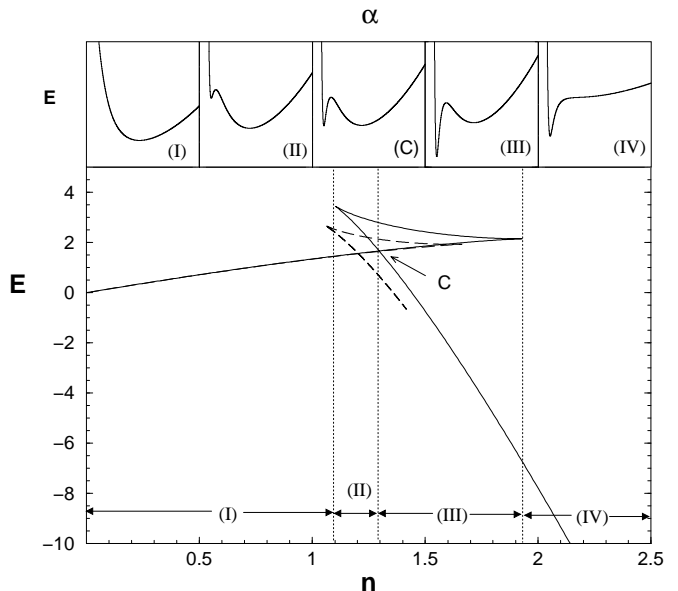


FIG. 1. In the lower part, we have a comparison between variational (solid curve) and exact (dashed curve) numerical calculations of the condensate energy as a function of the reduced number of atoms n for $g_3 = 0.005$. In the upper part we show five plots of the variational energy as a function of the variational parameter α for five particular values of n shown also in the lower frame. (I) (resp IV) corresponds to a small (large) n region where only one stable solution is encountered; (II) (resp III) to a small (large) n region where we observe three extrema for the energy; (C) corresponds to a particular n where we obtain two stable solutions with the same energy $E_1 = E_2$. E is given in units of $(N\hbar\omega)/n$.

In Fig. 1, we first illustrate the variational procedure considering an arbitrarily small three-body interaction, chosen as $g_3 = 0.005$. In the upper part of the figure, we show five small plots for the total variational energy E , in terms of the variational width α . Each one of the small plots corresponds to particular values of n . For each number n we report the energy of the variational extrema in the lower part of Fig. 1. In region (I) where the number of atoms is still small, the attractive two body force dominates over the repulsive three-body force and just one minima of the energy as a function of the variational parameter α is found. That is also the case for $g_3 = 0$. When the number of atoms is further increased (region (II)) two minima appear in the energy $E(\alpha)$. An unstable maximum is also found between the two minima. The lower energy minimum is stable while the solution corresponding to the smaller α is metastable. This solution has a higher density and, consequently, its metastability is justified by the repulsive three-body force acting at higher densities. The minimum number n for the appearance of the metastable state is characterized by an inflection point in the energy as a function of α . The value of n at the inflection point corresponds to the beak in the plot of extremum energy versus n because for larger n three variational solutions are found as de-

pictured in the lower part of Fig. 1. The attractive two-body and trap potentials dominate the condensed state in the low-density stable phase up to the crossing point (C). At this point, the denser metastable solution becomes degenerate in energy with the lower-density stable solution and a first order phase transition takes place. Since the two solutions differ by their density this transition is analogous to a gas-liquid phase transition for which the density difference between the liquid and the gas is the order parameter. In the variational calculation this occurs at the transition number $n \approx 1.3$ while the numerical solution of the NLSE gives 1.2. In region (III), we observe two local minima with different energies, a higher-density stable point and a lower-density metastable point. The metastable solution disappears in the beak at the boundary between region (III) and (IV). In regions (III) and (IV) the three-body repulsion stabilized a dense solution against the collapse induced by the two-body attraction. The qualitative features of the variational solution is clearly verified by the numerical solution of the NLSE, as shown by the dashed curve.

B. Numerical Results

The numerical solutions of Eq. (11) are obtained for several values of β , using three values of g_3 to characterize the solutions. We have used the Runge-Kutta (RK) and “shooting” method to obtain the corresponding solutions in each case [30]. The stability assignment for the stationary solutions was made by studying the corresponding time dependent Schrödinger equation, using the Crank-Nicolson (CN) method (see Refs. [11] and [31]). The numerical procedure to determine such stability was done in the following way: when applying the CN method, we started by using the static solution obtained from the RK method and observed if the modulus of the wave function remained constant. If this was occurring for a long period of time (of about 500 units of dimensionless time $\tau = \omega t$) the solution was considered stable, otherwise unstable.

In Fig. 2 we present the total energy as a function of the number of atoms, represented by the reduced number n defined in Eq. (13), for three significative values of the quintic parameter g_3 , given by 0, 0.016 and 0.03. The results agree with Ref. [15]. When $g_3 = 0$, the stable solutions for the energy starts at zero (for $n = 0$) and reaches a critical limit at $n_{max} \simeq 1.62$. There is no solutions for higher n , but the plot also shows a branch with unstable solutions (with higher energies) for $n \leq 1.62$. Our results are consistent with results given in Ref. [27]. When $g_3 = 0.03$, only stable solutions appear for the energy, with no limit in the number of atoms, having a maximum at $n \sim 2$. So, this and higher values for g_3 already represent a dominance of the quintic term in the interaction of Eq. (11). We observe that the numerical stability analysis is consistent with the variational ap-

proach discussed in the previous sub-section. The more interesting case represented in Fig. 2 is for $g_3 = 0.016$, as in such a case we observe a region of the plot where we can have up to three solutions for the same n . The inset to this figure amplifies the region of the plot where, for $g_3 = 0.016$, the solutions become unstable (between A and B) or metastable (between A and C, or B and C). At the point C a phase transition occurs from a less denser (gas) to a more denser (liquid) phase.

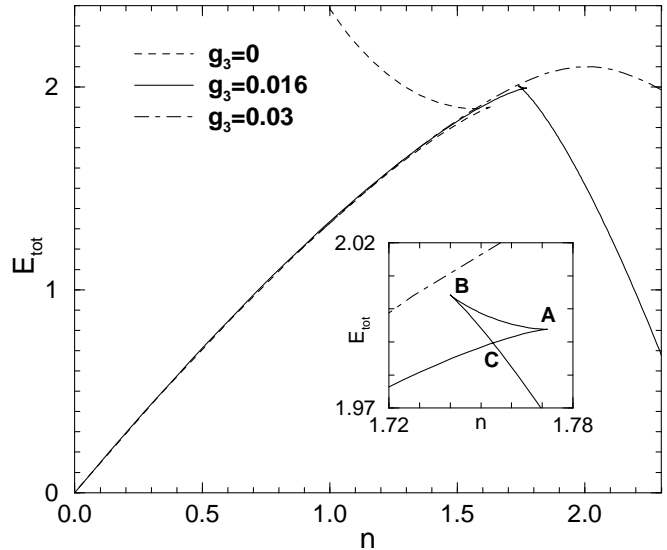


FIG. 2. The total energy, in units of $(\hbar\omega)/(2|a|\sqrt{2m\omega}/\hbar)$, is shown as a function of the reduced number of atoms n , given by Eq. (13), for $g_3 = 0, 0.016$ and 0.03 . The inset points out critical limits discussed in the text.

In Fig. 3, following a correspondence to Fig. 2, we present the results for the chemical potential in dimensionless units (β) as a function of n . The line with arrow in the inset to this figure indicates the approximate position in n , where the phase-transition (from a ‘gas’ phase to a ‘liquid’ phase) occurs. For $g_3 = 0.016$ the part of the plot linking points A and B is unstable (see both Figs. 2 and 3), otherwise it is stable. Finally, for $g_3 = 0.03$, the function of the energy in terms of n is always single valued and stable. Our calculation for $g_3 = 0$ also agrees with results presented in Ref. [11], with the maximum number of atoms limited to $n_{max} \approx 1.62$ [‡]. As we can see, for $n \leq n_{max}$ two solutions are possible, one of them being unstable. For g_3 higher than zero, a new pattern appears. For instance, the plot for the case of $g_3 = 0.016$ (see the inset) can be divided in several sectors according to the stability analysis, with the help of Fig. 2: Starting from $n = 0$ ($\beta = 1.5$) until point C_G, and from C_L

[‡]Our n is equal to $|C_{nl}^{3D}|$ of Ref. [11].

to higher values of n , we have stable solutions; from C_G to A and from B to C_L we obtain metastable solutions; from A to B the solutions are unstable, corresponding to maxima for the energies.

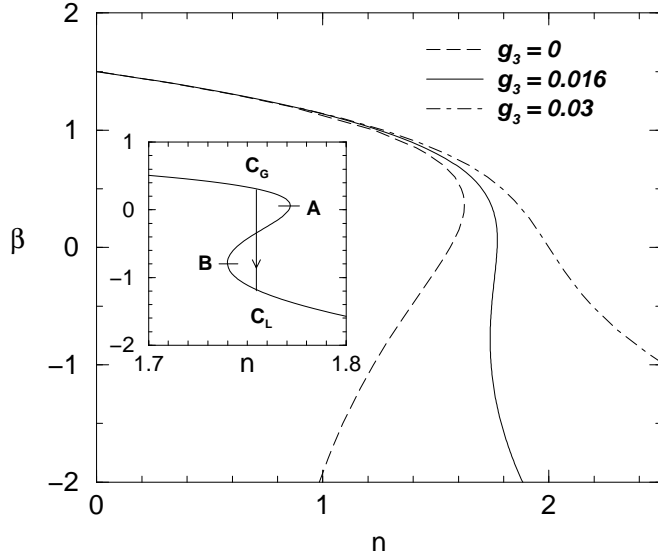


FIG. 3. The chemical potential, in dimensionless units ($\beta = \mu/(\hbar\omega)$), is shown as a function of the reduced number of atoms n , for the same set of g_3 shown in Fig. 2. The inset points out the critical limits corresponding to Fig. 2 (C_G and C_L corresponds to C), and the straight line with arrow indicates the transition from a less denser to a more denser phase.

In Fig.4 we also plot the central density ρ_c , defined in Eq. (10), as a function of the number n . We use the same values of the parameter g_3 as used in Figs. 2 and 3. The inset to the figure also points out the phase transition which occurs when $g_3 = 0.016$. As the transition the system becomes more than three times denser than the original one. Also, for $0 < g_3 < 0.0183$, we observe that the density ρ_c presents back bending typical of a first order phase transition.

By extending the observations of a first order phase transition, given in Figs. 2-4 for $g_3 = 0.016$, we also determined the region of g_3 where such kind of phase-transition can occur. In Fig. 5 we have a phase-diagram, where it was shown the critical boundary separating the two phases and a critical point at $n = 1.8$ and $g_3 = 0.0183$. For g_3 less then such critical value, we observe two regions with distinct phases, similar to gas and liquid phases. These two different phases are also clearly identified in our Fig. 4, where we present the central density as a function of n .

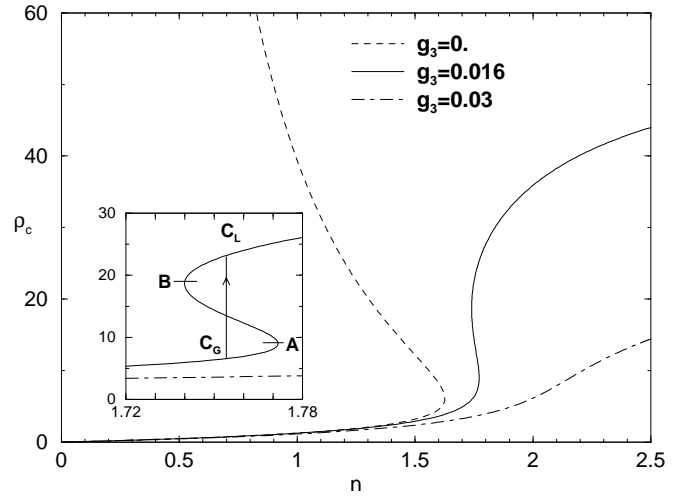


FIG. 4. Central density, in dimensionless units, as a function of the number n , for the same set of parameters g_3 given in Figs. 2 and 3.

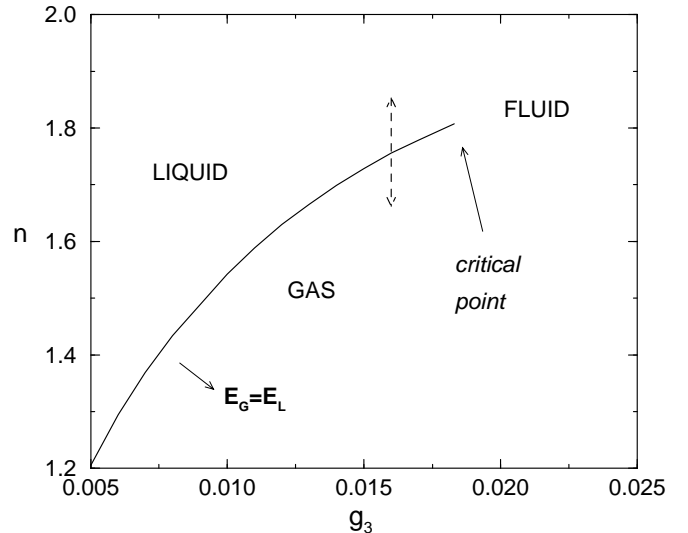


FIG. 5. Graphical representation of the interface of the two distinct phase (gas and liquid), in the plane defined by the reduced number of atoms n and the parameter g_3 (lower frame); and for the central density ρ_c versus g_3 (upper frame). The arrows in the lower frame correspond to the point where it occurs the phase transition for $g_3 = 0.016$, when changing n .

For each g_3 , the transition point given by the crossing point in the E versus n (see Fig. 2) corresponds to a Maxwell construction in the diagram of μ versus n . At this point an equilibrated condensate should undergo a phase transition from the branch extending to small n to the branch extending to large n . The system should never explore the back bending part of the diagram because, as seen in Fig. 2, it is an unstable extremum of the energy. From Figs. 1-5, it is clear that the first branch is associated with small densities, large radii, and positive chemical potentials while the second branch presents a more compact configuration with a smaller radius a

larger density and a negative chemical potential. This justifies the term gas (G) for the first one and liquid (L) for the second one. However we want to stress that both solutions are quantum fluids.

IV. COLLECTIVE EXCITATIONS

In this section, from the time evolution of GPG equation, given in Eq. (6), we consider the ground-state collective excitations for the system [32–34]. Following Ref. [34], the collective excitations are described by the Bogoliubov equations [4,25,29,35]. After including three body interactions they take the form

$$\begin{aligned} [\mathcal{L}_\nu - \hbar\omega_\nu]u_\nu + \{NU_0 + 2\lambda_3 N^2 |\psi_g|^2\} [\psi_g]^2 v_\nu &= 0 \\ [\mathcal{L}_\nu + \hbar\omega_\nu]v_\nu + \{NU_0 + 2\lambda_3 N^2 |\psi_g|^2\} [\psi_g^*]^2 u_\nu &= 0, \end{aligned} \quad (21)$$

where

$$\mathcal{L}_\nu \equiv H_0 - \mu + 2U_0 N |\psi_g|^2 + 3\lambda_3 N^2 |\psi_g|^4. \quad (22)$$

H_0 is the harmonic oscillator hamiltonian, $U_0 \equiv -(4\pi\hbar^2|a|)/m$, ω_ν is the frequency of the collective oscillations, N is the number of atoms and $\psi_g \equiv \psi_g(\mathbf{r})$ is the ground state solution of the Eq. (7). The above equations have been solved by using several methods [33,34,36]. In the present calculations we have employed two methods: a time-dependent and a time-independent one. In the time-dependent procedure we have added a weak perturbation to the potential and, with CN algorithm, examined the time evolution of Eq. (6) for a selected point of the wave-function. The lowest collective oscillations (ω_ν) were determined through Fourier transformation [34]. By using the time independent algorithm, we have solved Eqs. (21) with the matching algorithm [37] generalized for two functions u and v . The method works by departing from the analytically known u, v and ω_ν for the harmonic oscillator (chemical potential near to $3/2\hbar\omega$). Then we successively apply the matching method for the coupled u and v , gradually decreasing the chemical potential. This allows to reach subsequent solutions, by employing the deformation algorithm described in Ref. [30]. We obtain exact agreement between both methods, time-dependent or time-independent one.

Figure 6 shows the collective frequencies ω_ν as a function of n for the first mode ($l = 0$). The solutions corresponding to $g_3 = 0$ agree well with the ones given in Ref. [33], losing stability as $\omega_\nu \rightarrow 0$. By using this criterium, we have obtained the regions of stability for $g_3 = 0.016$. For $g_3 = 0.03$ all the solutions are stable. Following the inset of Fig. 6, for $g_3 = 0.016$, one can observe that, as the number of atoms is increased, in the less denser phase, the frequency of the collective excitations decreases and are related to stable solutions till the point C_G ; from this point down to the point A (increasing n), the frequency continues to decrease to zero, but now related to meta-stable solutions. As already explained previously in the discussion of Figs. 2-5, and also

from the variational energy solutions given in Fig. 1, it is very likely that occurs a phase transition, from C_G to C_L (or from the meta-stable solutions, given in the branches C_G-A and $B-C_L$, to the corresponding stable solutions with fixed n). Once in the denser phase (from B passing through the point C_L), the frequency of the collective excitations increases as the number of atoms increases, contrary to the behavior observed for the system in the less denser phase. This can be qualitatively understood considering the variational energy of the two phases and the corresponding stable energy as shown in Fig. 1. The curvature of the variational energy as a function of α at the minimum for the liquid phase is bigger than the corresponding one in the gas phase [compare in Fig.1 the insets (I) and (II) with the insets (III) and (IV)]. This indicates, in agreement with Fig. 6, that the restoration force is stronger for the liquid phase than for the gas phase and consequently the frequencies of the collective modes starting at the point C_L are higher than the corresponding ones for the gas phase ending at C_G . As we include more particles the frequencies of the oscillations increase in the liquid phase. Corresponding to Fig. 6, in Fig. 7 the collective frequencies are shown as a function of the chemical potential β . From right to left, as the chemical potential decreases till C_G , β also decreases; from C_G to A, and from B to C_L the solutions are meta-stable, such that the system will look for a transition to a stable branch (from C_G , increasing β , and from C_L , decreasing β). From C_L , as we further decreases the value of β the frequency of the collective excitations increases.

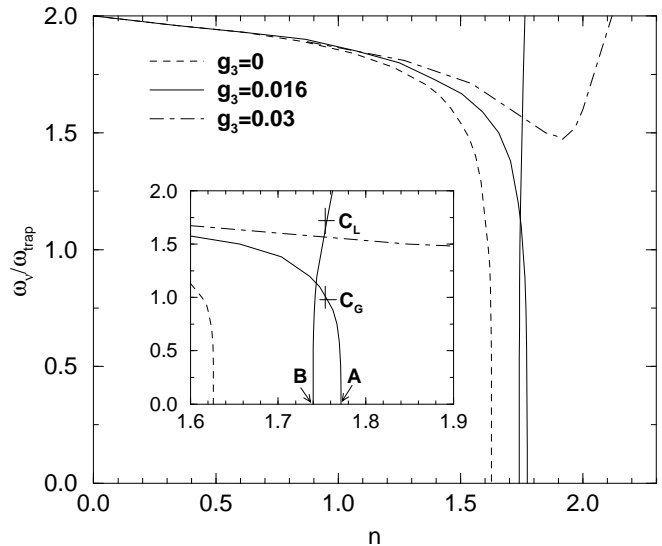


FIG. 6. Collective frequencies as a function of the reduced number of atoms n . The inset shows the critical points corresponding to the previous figures.

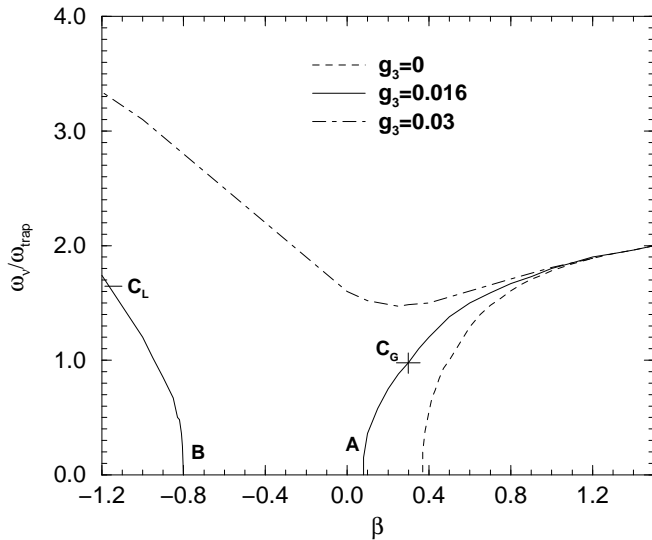


FIG. 7. Collective frequencies as a function of the chemical potential β .

V. CONCLUSIONS

To summarize, we have presented results for the total energy, chemical potential, central density, in terms of the number of atoms in the condensed state, for a range of values of the three-body strength. We also study the lowest collective mode excitations of the ground-state. Our calculation presents, at the mean-field level, the consequences of a repulsive three-body effective interaction for the Bose condensed wave-function, together with an attractive two-body interaction. A first-order liquid-gas phase-transition is observed for the condensed state as soon as a small repulsive effective three-body force is introduced. In dimensionless units the critical point is obtained when $g_3 \approx 0.0183$ and $n \approx 1.8$. The characterization of the two-phases through their energies, chemical potentials, central densities and radius were also given for several values of the three-body parameter g_3 . The results presented in this paper can be relevant to determine a possible clear signature of the presence of repulsive three-body interactions in Bose condensed atoms. It points to a new type of phase transition between two Bose fluids. Because of the condensation of the atoms in a single wave-function this transition may present very peculiar fluctuations and correlations properties. As a consequence, it may fall into a different universality class than the standard liquid-gas phase transition, which are strongly affected by many-body correlations. This matter certainly deserves further studies.

Acknowledgments

This work was partially supported by Fundação de Amparo à Pesquisa do Estado de São Paulo and Conselho Nacional de Desenvolvimento Científico e Tecnológico.

- [1] S.N. Bose, Z. Phys. **26**, 178 (1924); A. Einstein, Sitz. Preuss Acad. Wiss. **261** (1924); 3 (1925).
- [2] A.S. Parkins and D.F. Walls, Phys. Rep. **303**, 1 (1998); A. Griffin, D.W. Snoke, and S. Stringari, *Bose-Einstein Condensation* (Cambridge University Press, Cambridge, 1995).
- [3] F. London, Phys. Rev. **54**, 947 (1938); F. London, *Superfluids II* (John Wiley and Sons, New York, 1954).
- [4] N.N. Bogoliubov, J. Phys. (USSR) **11**, 23 (1947).
- [5] M.H. Anderson, J.R. Ensher, M.R. Matthews, C.E. Wieman, E.A. Cornell, Science **269**, 198 (1995).
- [6] C.C. Bradley, C.A. Sackett, J.J. Tollet and R.G. Hulet, Phys. Rev. Lett. **75**, 1687 (1995); C.C. Bradley, C.A. Sackett and R.G. Hulet, Phys. Rev. Lett. **78**, 985 (1997); C.C. Bradley, C.A. Sackett, J.J. Tollet and R.G. Hulet, Phys. Rev. Lett. **79**, 1170 (1997).
- [7] K.B. Davis, M.-O. Mewes, M.R. Andrews, N.J. van Druten, D.S. Durfee, D.M. Kurn, W. Ketterle, Phys. Rev. Lett. **75**, 3969 (1995); M.R. Andrews, M.-O. Mewes, N.J. van Druten, D.S. Durfee, D.M. Kurn, W. Ketterle, Science **273**, 84 (1996); M.-O. Mewes, M.R. Andrews, N.J. van Druten, D.M. Kurn, D.S. Durfee, and W. Ketterle, Phys. Rev. Lett. **77**, 416 (1996).
- [8] D.G. Fried, T.C. Killian, L. Willmann, D. Landhuis, A.C. Moss, T.J. Greytak, and D. Kleppner, Phys. Rev. Lett. **81**, 3811 (1998).
- [9] E. Cornell, J. Res. Natl. Inst. Stand. Technol. **101**, 419 (1996).
- [10] K. Huang, *Statistical Mechanics*, 2nd. edition (John Wiley and Sons, New York, 1987).
- [11] M. Edwards and K. Burnett, Phys. Rev. **A51**, 1382 (1995); P.A. Ruprecht, M.J. Holland, K. Burnett, and M. Edwards, Phys. Rev. **A51**, 4704 (1995).
- [12] G. Baym and C.J. Pethick, Phys. Rev. Lett., **76**, 6 (1996).
- [13] J. Weiner, V.S. Bagnato, S. Zilio, and P.S. Julienne, Rev. Mod. Phys., **71**, 1 (1999).
- [14] Yu. Kagan, A.E. Muryshev, G.V. Shlyapnikov, and J.T.M. Walraven, Phys. Rev. Lett. **76**, 2670 (1996).
- [15] N. Akhmediev, M.P. Das and A.V. Vagov, Int. J. Mod. Phys. **B13**, 625 (1999).
- [16] A. Gammal, T. Frederico, and L. Tomio, *Trapped Bose-Einstein condensed gas with two and three-atom interactions*, in proceedings of the "International Workshop on Collective Excitations in Fermi and Bose Systems", ed. by C. Bertulani, L.F. Canto and M. Hussein (World Scientific, Singapore, 1999).
- [17] B.D. Esry, C.H. Greene, Y. Zhou, and C.D. Lin, J. Phys. **B 29**, L51 (1996).
- [18] C. Josseland and S. Rica, Phys. Rev. Lett. **78**, 1215 (1997).
- [19] Yu. Kagan, B.V. Svistunov, and G.V. Shlyapnikov, JETP Lett. **42**, 209 (1985).
- [20] P.O. Fedichev, M.W. Reynolds, and G.V. Shlyapnikov, Phys. Rev. Lett. **77**, 2921 (1996).
- [21] E.A. Burt, R.W. Ghrist, C.J. Myatt, M.J. Holland, E.A. Cornell, and C.E. Wieman, Phys. Rev. Lett. **79**, 337 (1997).
- [22] V. Efimov, Phys. Lett. **B 33**, 563 (1970); Comm. Nucl. Part. Phys. **19**, 271 (1990).

- [23] T. Frederico, L. Tomio, A. Delfino, and A.E.A. Amorim, Phys. Rev. **A60**, R9 (1999).
- [24] V.L. Ginzburg and L.P. Pitaevskii, Zh. Eksp. Teor. Fiz. 34, 1240 (1958) [Sov. Phys. JETP 7, 858 (1958)]; E.P. Gross, J. Math. Phys. 4, 195 (1963).
- [25] L.P. Pitaevskii, Zh. Éksp. Teor. Fiz. **40**, 646 (1961) [Sov. Phys. JETP 13,451 (1961)].
- [26] A.E.A. Amorim, T. Frederico, and L. Tomio, Phys. Rev. C **56**, R2378 (1997).
- [27] M. Houbiers and H.T.C. Stoof, Phys. Rev. A **54**, 5055 (1996).
- [28] A.L. Fetter and J.D. Walecka, *Quantum Theory of Many - Particle Systems* (McGraw-Hill, New York, 1971).
- [29] A.L. Fetter, Phys. Rev. A**53**, 4245 (1996).
- [30] A. Gammal, T. Frederico, and L. Tomio, Phys. Rev. **E60**, 2421 (1999).
- [31] W.F. Ames, *Numerical Methods for Partial Differential Equations*, 3rd. ed., Academic Press, New York, 1992, pp. 111-115.
- [32] S. Stringari, Phys. Rev. Lett. **77**, 2360 (1996).
- [33] K.G. Singh and D.S. Rokhsar, Phys. Rev. Lett **77**, 1667 (1996).
- [34] P.A. Ruprecht, M. Edwards, K. Burnett, and C.W.Clark, Phys. Rev. A **54**, 4178 (1996); M. Edwards, P.A. Ruprecht, K. Burnett, R.J. Dodd, and C.W. Clark Phys. Rev. Lett. **77**, 1671 (1996).
- [35] A.L. Fetter, Ann. Phys. (N.Y.) **70**, 67 (1972); A.L. Fetter and D. Rokhsar, Phys. Rev. **A57**, 1191 (1998).
- [36] L. You, W. Hoston and M. Lewenstein, Phys. Rev. A **55**, R1581 (1997).
- [37] N.J. Giordano, *Computational Physics*, Prentice-Hall, New Jersey, 1997, pp. 257-272.